DEPOSITION AND EVALUATION OF SILICON FILMS

FORMED BY PYROLYTIC DECOMPOSITION OF SILANE ON OXIDIZED

SILICON SINGLE CRYSTALS

A Thesis

Presented to

the Faculty of the School of Engineering and Applied Science

University of Virginia

In Partial Fulfillment

of the Requirements for the Degree

Master of Materials Science

by

Archibald Linley Fripp, Jr.

June 1969

APPROVAL SHEET

This thesis is submitted in partial fulfillment of

the requirements for the degree of

Master of Materials Science

_____
Author

Approved:

_____
Faculty Advisor

_____
Dean, School of Engineering and
Applied Science

June 1969

ACKNOWLEDGMENTS

TABLE OF CONTENTS

LIST OF TABLES

LIST OF FIGURES

LIST OF SYMBOLS

cc   cubic centimeter

μ micron (10^{-6} meter)

$\overset{o}{A}$ angstrom unit (10^{-10} meter)

θ angle between X-ray beam and sample surface

cps   counts per second

σ_{hkl} percentage of surface covered with crystals whose hkl planes are parallel to the substrate

I   intensity

R.I.   relative intensity

ABSTRACT

The chemical deposition of silicon on thermally grown silicon dioxide has been investigated. The reactant was semiconductor grade silane (SiH_4) in an induction heated hydrogen flow system. The deposit was found to be polycrystalline with a strong (110) preferred orientation which tended toward a random orientation at high temperatures. A geometrical model, based on the possible second near the neighbor positions of silicon atoms in the amorphous silicon dioxide, is proposed which offers an explanation for the strong (110) orientation for moderate temperatures and the near random orientations for high temperatures.

CHAPTER I

INTRODUCTION

This thesis is part of an investigation undertaken to determine
the feasibility of using the pyrolytic decomposition of silane (SiH$_4$) to
deposit polycrystalline silicon on thermally oxidized silicon substrates
which are to be used in manufacturing dielectrically isolated integrated
circuits. The basic process of dielectric isolation has been reported
by TRW,[1] Maxwell, Beeson, and Allison,[2] and Jackson,[3] by which tiny
islands of single crystal silicon are electrically isolated from each
other by silicon dioxide and the entire structure is supported by
polycrystalline silicon which has been deposited on the silicon dioxide
surface. Figure 1 is a schematic of the dielectric isolation process.
Integrated circuits built by this process have better high-frequency
characteristics and are more radiation resistant than conventional
integrated circuits.

The objective of this paper is to investigate the effect of
substrate temperature on the preferred crystallographic orientation of
the deposited silicon and to determine if the presence of etched channels
in the otherwise planar substrate surface produces any undesirable
effects. The electrical characteristics of the dielectrically isolated
silicon islands will be reported in a later paper.

A brief discussion of film deposition in general is presented in
chapter 2 of this thesis along with a literature review of previous work
done on silicon deposition. The topics reviewed include the physical

A   A'

Si O_2

Silicon Crystal

Oxidized Silicon Wafer

Expanded AA' View

(a) Etch Pattern in Oxide

SiO_2

Silicon Crystal
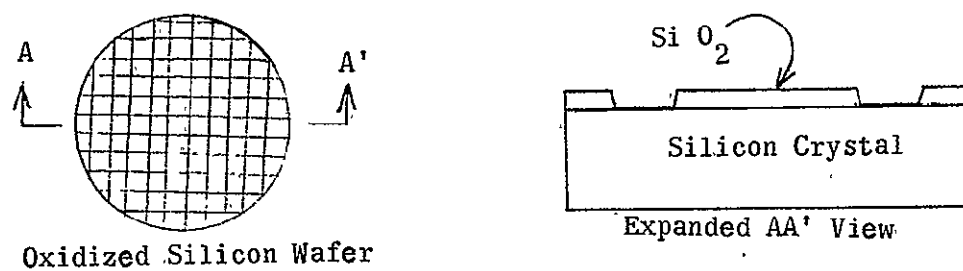
Deposited Silicon
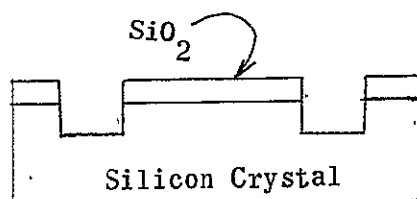
Crystal

(b) Etch Silicon Crystal

(c) Deposit Silicon

Crystal SiO_2
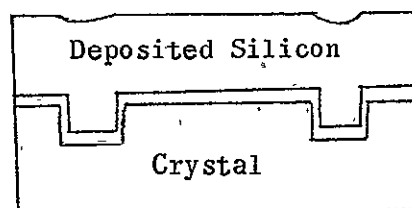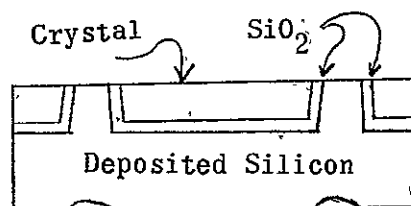
Deposited Silicon

(d)-Lap Crystal, Invert, and Process for Active Elements

Figure 1.-Processing Steps in Dielectric Isolation.

and chemical deposition of silicon on amorphous substrates as well as silicon deposition on silicon and on crystalline (α-quartz) silicon dioxide. Silicon-on-silicon epitaxy is reviewed only where silane was the source material.

Surface texture is reported for the physically deposited films and for one case of the chemically deposited films in which silane was used to deposit silicon on fused (amorphous) quartz. In the silane deposition[4] all deposits were found to be randomly orientated which is in contrast to the texture of the vacuum deposited films. No information has been reported on the microstructure of silicon deposited by the pyrolysis of silane on thermally oxidized silicon substrates.

The experimental system and the various steps taken to produce and evaluate the polycrystalline silicon films are discussed in chapter 3. Particular attention is given the silane-hydrogen reaction system in which silane decomposes to produce elemental silicon.

Chapter 4 discusses the experimental results as evaluated with the aid of X-ray diffraction and scanning electron microscopy. A model is proposed in this chapter to give the relative percentage of the substrate surface which is preferentially covered by one of the low index crystallographic planes. The samples are characterized by the percentage of preferred orientation as a function of substrate temperatures.

The final chapter makes an extrapolation of Bicknell's[5] model for epitaxial deposition of silicon on α-quartz to explain the experimental

results. The proposed theoretical model produces a preferred orientation in the deposit at moderate temperatures and a random orientation at high temperatures.

CHAPTER II

LITERATURE REVIEW AND GENERAL THEORY

General Theory

The silicon atoms which are deposited are obtained from the

pyrolytic decomposition of silane gas (SiH_4) in a hydrogen atmosphere.

Decomposition of silane begins at 400° C and increases with increasing

temperature.[6] The decomposition process is thought to take place by a

heterogeneous reaction in which the silane molecules are absorbed on the

substrate surface, break down to form one silicon atom and two hydrogen

atoms per silane molecule; the hydrogen atoms are desorbed back into the

gas stream and the silicon is left free on the substrate surface. The

absorbed silicon atom may either attach itself to a stable nucleus and

grow, combine with another atom or critical nucleus to form a stable

nucleus, or it may evaporate.[7]

In the case of a substrate surface having free bonds (as is likely

with silicon dioxide in the highly reducing environment of a hydrogen

atmosphere at high temperature, where both previously deposited silicon

atoms and hydrogen atoms may capture surface oxygen atoms leaving

silicon bonds exposed on the substrate surface) it is also possible that

the silicon adatom may bond directly to the substrate. In this case,

the nuclei may be expected to form in a preferred orientation which

would depend on the number and spacing of the substrate bonds.

Even if the nuclei form in a preferred manner, the final orienta-

tion of the film may have an orientation different from that of the

5

nuclei. That is, the substrate surface may lead to a preferred

nucleation orientation but growth conditions may be such that these

nuclei cannot grow while other orientations may be in favorable growth

conditions.[8]

Literature Review

1. Physical Deposition of Silicon on Amorphous Substrates

   A. Vacuum Evaporation

F. M. Collins[9] evaporated silicon from a resistance heated boron

nitride crucible onto heated fused quartz substrates. Experiments were

carried out in 1 to 5×10^{-6} torr vacuum with substrate temperatures

ranging from 400° C to 1100° C. Film thickness was on the order of one

micron.

Crystallinity was measured with an X-ray diffractometer. The

films were amorphous for substrate temperatures below 550° C.

Crystallinity, that is, the intensity of recorded X-ray peaks for constant

X-ray flux, increased with increasing substrate temperature with a

preferred (111) orientation becoming apparent, and increasing, at 1000° C.

Y. Kataoka[10] evaporated silicon from tantalum filaments onto fused

quartz substrates heated to 950-1050° C. The vacuum of the system was

maintained at pressure between 5 to 10×10^{-6} torr and the deposition

rate was approximately 0.6 u/min for films 3.5μ thick. The

crystallography of the film was measured by X-ray diffraction, and the

deposits were found to have a (111) preferred orientation.

A. J. Mountvala and G. Abowitz[11] evaporated silicon with an electron beam in 1×10^{-6} torr vacuum for deposition rates of between 0.002 μ/min and 0.08 μ/min. The fused quartz substrates were heated to temperatures ranging from 500 to 1000° C and the films ranged in thickness from 0.05μ to 0.75μ. The textural characteristics of the deposited films were measured by X-ray diffraction and were found to vary from an amorphous structure for substrate temperatures below 700° C, increasingly strong (110) texture between 765° C and 900° C, and a texture going from (110) to (111) at 1000° C. Surface topology was viewed with a 50X optical microscope to show regions, on the same substrate, of widely varying grain sizes. The grains were about 50μ diameter in one region, 160μ diameter in another, and were rectangles, with dimensions of several hundred by over 1000μ, in the third region. Electron microscopy (19,000X) pictured a rough surface which was thought to be caused by thermal etching of the substrate.

R. G. Breckenridge and coworkers[4] deposited silicon films on heated fused quartz by using electron beam evaporation in 2×10^{-7} torr vacuum. Substrate temperatures ranged from 800-1000° C and the deposition rate was approximately 0.009 μ/min for films 0.4 to 1.16μ thick. The surface texture ranged from random orientation at a deposition temperature of 800° C, preferred (100) orientation at 900° C, and preferred (111) orientation at 1000° C.

B. Sputtered Films

H. Y. Kumagai, J. M. Thompson, and G. Kraus[12] deposited silicon films on heated fused quartz substrates by sputtering in an argon

atmosphere. All films investigated were deposited at 0.01 μ/min for thicknesses of 0.1, 1.0, and 4.0μ. Electron diffraction of the 0.1μ films and X-ray diffraction of the 1.0 and 4.0μ films showed an almost amorphous structure for substrate temperatures up to 400° C during deposition but post heat treatments above 650° C produced a strong polycrystalline structure; however no preferred orientation was found for post heat treatments as high as 1000° C.

2. Chemical Deposition of Silicon on Amorphous Substrates

A. Hydrogen Reduction of Trichlorosilane (SiHCl₃)

TRW[1] used an oxidized silicon single crystal wafer as a substrate for silicon deposition from SiHCl₃. Hydrogen (flow rate = 2000 cc/min) was used as a carrier gas and silicon was deposited at 4 μ/min with substrate temperature of 1100° C. The final film thickness was approximately 150μ. This report gave no information on the microstructure of the deposited films.

B. Hydrogen Reduction of Silicon Tetrachloride (SiCl₄)

E. G. Alexander and W. R. Runyan[13] made depositions of silicon on thermally oxidized single crystal silicon by hydrogen reduction of SiCl₄ near 1200° C. In the early stages of growth octahedral silicon crystals, 1 to 50μ diameter, were observed on the silicon dioxide surface. These investigators stated that impurities on the oxide surface aided the nucleation of silicon growth, the use of a sodium salt (such as $Na_2H_2PO_2 \cdot H_2O$) was needed for a uniform deposit, and that hydrogen reduction of the SiO₂ surface may be instrumental in forming

nuclei on the untreated wafers. No information was reported on preferred orientation or final topology of the deposited silicon.

E. G. Bylander and M. M. Mitchel[14] deposited silicon on fused quartz in the temperature range of 950-1200° C by hydrogen reduction of silicon tetrachloride. It was noted that silicon first nucleated at etched areas on the quartz and a typical growth included many octahedral silicon crystallites on the substrate surface.

C. Pyrolysis of Silane (SiH_4)

R. G. Breckenridge and coworkers[4] deposited silicon on fused quartz by the pyrolytic decomposition of SiH_4. Using substrate temperatures of 900-1300° C and flow rates of 5 to 40 ml/min only randomly oriented layers were produced. No other information about microstructure was included.

In studies of silicon nucleation on silicon substrates Joyce and Bradley[15] used a molecular beam of silane molecules incident upon the interface of single crystal silicon and oxidized silicon. After 240 minutes, surface examination revealed nucleation centers growing on the crystal but no growth on the oxide. It was concluded that at the low growth rates (9.3×10^{15} molecules cm^{-2} sec^{-1}) used in the experiment no growth occurs on the oxide surface.

3. Epitaxial Silicon on Single Crystal Substrates by the Pyrolysis of Silane (SiH_4)

A. Single Crystal Silicon Substrates

Using very low growth rates (approximately 1.0 A/min or 10^{-4} μ/min) in a silane molecular beam deposition system, Booker and Joyce[16] showed

that nucleation of silicon began as separate growth centers, usually separated by a few microns, at random sites on the substrate which was heated to 845° C. The nuclei were shaped as truncated tetrahedra on the (111) orientated silicon substrate with approximately 4 to 1 base-to-height ratio. The three inclined sides of the tetrahedra intersected the substrate along the three < 110 > directions. These nuclei continued to grow with time and it was assumed that they would ultimately have joined to give a continuous epitaxial layer.

Using the same molecular beam system, Joyce, Bradley, and Watts[17] investigated the nucleation of pyrolytically decomposed silane on (100) silicon substrates. Again silicon growth started as separate growth centers which were rectangular in shape.

The data for both nucleation experiments were fitted to the theory of Lewis and Campbell[7] to predict a minimum (111) nucleus of three atoms and a minimum (100) nucleus of four atoms. However, when the silicon substrates were given an extensive predeposition cleaning treatment no nuclei growth was observed. Exposure of the clean wafers to organic contamination again produced three dimensional nucleation. It was concluded that the discrete growth centers were due to minute amounts of surface contamination.

The two papers (16 and 17) reviewed above investigated silane deposition only in the initial nucleation region. In earlier work Joyce and Bradley[18] investigated epitaxial silicon on silicon by using low partial pressures of silane in a previously evacuated system. Complete silicon overgrowths were observed for growth temperatures

between 920° C and 1260° C and silane pressure of 1 torr. The growth

rates as effected by substrate temperature and silane pressure are

listed in table I.

TABLE 1

Temperature range investigated	$920-1260^\circ$ C
Growth rate (μ/min) as affected by temperature	$920 < T < 1100^\circ$ C Exponential increase (activation energy = 37 K cal./mole) $T < 1100^\circ$ C G.R. = constant (for constant pressure)
Growth Rate (μ/min) Law as affected by SiH_4 pressure	$T < 1100^\circ$ C G.R. = $e^{ap} - 1$ for $0.1 < p < 1.5$ torr $T > 1100^\circ$ C G.R. = CP^n; n = 1.3 at 1060° C

S. E. Mayer and Shea[19] investigated the deposition rate

of silicon on silicon by the pyrolytic decomposition of silane using

a H_2-SiH_4 flow system instead of a vacuum system. The growth rate was

slightly temperature dependent with a maximum at 1200° C. Deposition

rates were also affected by the hydrogen-silane ratio, holding the flow

rate of hydrogen and substrate temperature constant; and by the SiH_4

flow rate, holding the H_2 - SiH_4 ratio and temperature constant.

Bhola and A. Mayer[20] also deposited epitaxial silicon films on single

crystal silicon substrates by the pyrolysis silane in a hydrogen silane

flow system. After diluting the silane to 0.2 volume percent in hydrogen they obtained deposition rates 0.8 μ/min for substrate temperatures of 1050 to 1070° C and 1.12 μ/min for temperatures of 1100 to 1140° C. The silicon layers tended to become polycrystalline for deposition temperatures below 1000° C.

B. Single Crystal Quartz Substrates

Bicknell, Charig, Joyce, and Stirland[5] grew epitaxial layers of silicon on the (01$\bar{1}$0), (11$\bar{2}$0), and (0001) faces of single crystal quartz using a hydrogen-trichlorosilane flow system. Electron microscopy showed growth nucleating as individual growth centers. The observation that the growth centers, or islands, were fairly constant in size regardless of their distribution density was interpreted to imply that the mobility of silicon atoms on the quartz surface was quite low and, hence, islands grow only by receiving new adatoms. The islands were almost 1000 Å thick before the final channels between islands disappeared.

As a "speculative" model for epitaxy it was proposed that in the reducing atmosphere (hydrogen at 950 to 1250° C) the quartz surface would be oxygen deficient which would produce free silicon bonds and bonding would occur at the silicon-silicon interface. This, theory was substantiated by experimental results in which the (001) face of silicon is parallel to (0001) quartz and (010) silicon is parallel to (10$\bar{1}$0) quartz for the three quartz orientations studied.

Part of this group of workers[21] later compared the above work with silicon on quartz epitaxy produced by a silane-vacuum system. For

both systems it was found that the growth rate of the epitaxial layer was essentially independent of substrate temperature (950 to 1250° C) but was a function of the partial pressure of the gas (trichlorosilane or silane) only. The comparison of the two gases did not go into the type, size, and distribution of nuclei.

Summary

Epitaxial deposition of silicon on single crystals has been extensively investigated and, although there is quite a bit of disagreement, the properties of silicon evaporated on fused quartz substrates has been reported for substrate temperatures varying from 400° C to 1100° C. There has been only one report of using the pyrolytic decomposition of silane to deposit silicon on fused quartz[4] and the results (random orientations for temperatures ranging from 900 to 1300° C) did not agree with any of the vacuum deposition reports. The author wishes to extend the knowledge of silicon deposits on amorphous substrates by investigating the effect of substrate temperature on the preferred orientation of silicon deposited by the pyrolytic decomposition of silane on thermally oxidized silicon wafers. To the author's knowledge there have been no previous reports of work in this immediate area.

CHAPTER III

THE EXPERIMENT

The broad purpose of this research was to investigate the use of
silane in depositing polycrystalline silicon on oxidized single crystal
silicon to be used in dielectrically isolated integrated circuits. The
immediate objective was to investigate the effect of substrate tempera-
ture on the preferred orientation of pyrolytically deposited silicon on
thermally oxidized single crystal silicon.

The basic steps in the experiment were:

1. Oxidation of the single crystal silicon wafers

2. For some wafers, etching of moats in crystal surface

3. Pyrolytic silane reaction for silicon deposition

4. X-ray diffraction examination for preferred orientation

5. Microscope examination, both optical and electron scanning

    microscopy, for surface topology

Each of these steps will be discussed under a separate heading.

1. Oxidized Silicon Substrate

The initial wafers were 0.005 ohm-cm boron doped single crystal
silicon orientated within 2° of the (111) face. The wafers were purchased
already sliced (1 in. $\times$ 0.01 in.), lapped, and polished. The substrates
were oxidized in a quartz tube furnace at 1100° C by bubbling nitrogen
(1000 cc/min) through a water bath heated to 91° C (partial pressure of
water vapor 525 torr). An oxidation time of 2 hours and 45 minutes
produced a one micron thick oxide. Since the color of a thin oxide

layer is due to light interference, the lack of color variation of the

oxide surface indicated that the layer was flat and smooth.

No structure determination measurements were performed on these

oxidized substrates but silicon dioxide grown on clean silicon substrates

has been reported as being amorphous with short range cristobalite

structure.[22,23] The β-cristobalite structure has silicon-silicon

interatomic spacings of 3.08 Å and 5.03 Å, and using electron diffraction

techniques the average spacing of silicon atoms in thermally grown

oxides has been measured as 3.10 Å.[29]

2. Formation of Channels in Silicon Crystal Surface

In order to simulate the dielectric isolation fabrication

technique, approximately one-half of the test substrates had channels

etched in the surface of the single crystal wafer. The channels were

approximately 0.005, 0.006, and 0.008 inches wide, 0.20 inches long, and

0.001 inches deep with the lengths of the channels both perpendicular

and parallel to direction of incoming gas flow (see Fig. 2).

In forming the channels the standard photo-resist technique was

used to etch the channel width and length through the oxide to the

silicon surface using a buffered HF solution (1 part (vol.) HF to

4 parts (vol.) of solution of 8 parts (wt.) NH_4F to 15 parts weight of

deionized water).[24] The photo-resist is removed and a solution

($HF:HNO_3:HAc;2:15:5$ (vol.))[1] which preferentially etches silicon and

not silicon dioxide is used to etch the moats to a depth of approximately

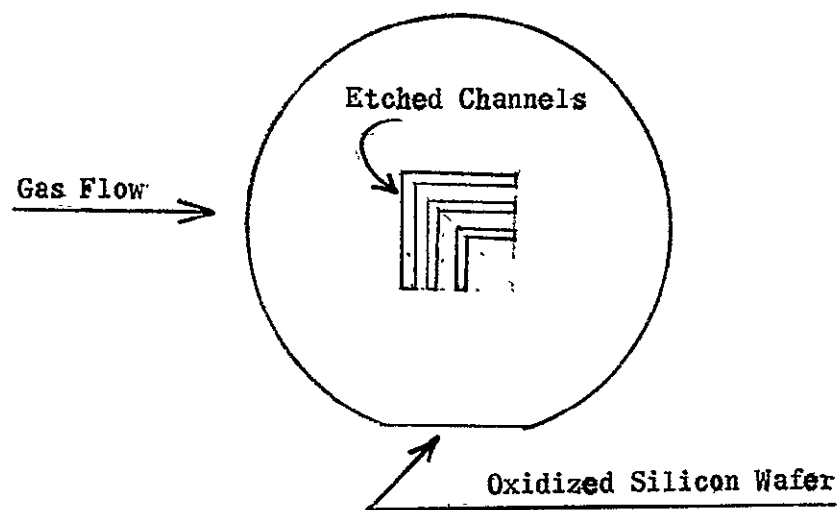0.001 inch. After etching the silicon, the remainder of the oxide is

Figure 2.- Test Pattern for Dielectric Isolation.

removed using the buffered HF solution. The etched wafer is then

processed (cleaned, oxidized, etc.) as a new wafer. The etching steps

are listed below:

Selective Area Etching of Silicon

a. Oxidize wafer (approximately 1μ of oxide)

b. Place wafer on spinner, apply KMER photo resist, spin at
3000 rpm for 30 seconds

c. Dry photo-resist for at least 10 minutes at 185° F in
vacuum oven

d. Place mask over wafer and expose photo-resist with sun lamp
(approximately 20 sec)

> The mask used in this step is a Kodak glass slide
> which is the negative photograph (20:1 reduction)
> of a plastic sheet. The plastic sheet is a two
> layer laminate, one layer is clear, the other is
> opaque. By carefully cutting and removing only
> the opaque layer any desired mask can be fabricated.

e. Develop exposures

f. Harden photo-resist in 185° F vacuum oven for at least
2 hours.

[The silicon dioxide is now completely covered with polymerized

photo resist except in the regions where the channels are to be

etched in the silicon crystal. The polymerized photo-resist is

strongly resistant to the buffered HF acid but it is readily

attacked by the silicon etching solution. Hence, the necessity

of using a two step masking technique.]

g. Etch the exposed oxide with the buffered HF solution

h. Remove the polymerized photo-resist with hot sulfuric acid
(H_2SO_4)

      i. Using the etched silicon dioxide as a mask, etch the channels

        · in the silicon crystal

      j. Remove the remainder of the oxide in buffered HF

      k. Reoxidize wafer as in part 1.

3. Silicon Deposition by the Pyrolytic Decomposition of Silane

    The experimental system used in this research was a Westinghouse induction heated silicon epitaxial growth system which is powered by a standard 15 kw-RF (460 KHz) generator. Gases used in the various reactions are stored in a cabinet behind the master gas flow control panel. The gases are fed through stainless steel tubing from the storage cylinders to electromechanical (solenoid) valves and are then metered through needle valve-controlled flow meters. The carrier gas, hydrogen, is first in line; it "picks up" and mixes the other gases through approximately 3 feet of tubing on the way to the reaction chamber. The gas flow times and sequences can be operated either manually or automatically, in which case the flow times are preset. In either case the gas flow rates and any temperature changes are manually controlled.

    The reaction chamber is a 30 × 2-1/2 inch fused quartz tube with ground fittings on each end. The gases are exhausted into a ventilated water scrubber.

    Substrates used for the various depositions are placed on either a silicon carbide coated graphite susceptor or a quartz envelope containing a graphite susceptor. In either case, the susceptor has dimensions of approximately 9-1/2 × 1-3/4 × 1/2 inch. The susceptor is heated by a water cooled RF induction coil. Temperature is set using a

standard optical pyrometer and is controlled by a two-color pyrometer.
Figure 3 is a block diagram and Figure 4 is a picture of the system.

In a typical run four wafers were placed on a silicon-carbide
coated graphite susceptor which was positioned inside the quartz reactor
tube at the midpoint of the RF induction coil, at an angle of approximately 7° from horizontal. The first and fourth wafers in line on the
susceptor were single crystals (no thermal oxide growth) in the "as
received" (i.e., lapped, chemically polished, and cleaned) condition;
the second wafer, usually, was an etched oxide coated sample, and the
third wafer was a planar oxide coated sample. Basically, wafers 2 and 3
were test samples, and wafers 1 and 4 were monitors. A doping gas, PH_3,
was added to the flow to aid evaluation of the monitors.

The gas flow lines and reactor tube were purged with nitrogen
and then hydrogen before activation of the RF generator. Once the RF
generator was activated the temperature rise time was very rapid (approx.
1 to 2 minutes to obtain desired, $800-1200^\circ$ C, temperature). During
warmup, temperature and gas flow rates were adjusted to desired values
(silane and doping gases were shunted around the reactor tube during
this period). At the end of the 8 minute warmup period the silane and
doping gas were switched into the reaction chamber and the pyrolytic
deposition began. At the end of the deposition time the silane and
doping gas flows were cut off and the temperature remained constant
for one minute, then the RF generator was cut off, and the samples were
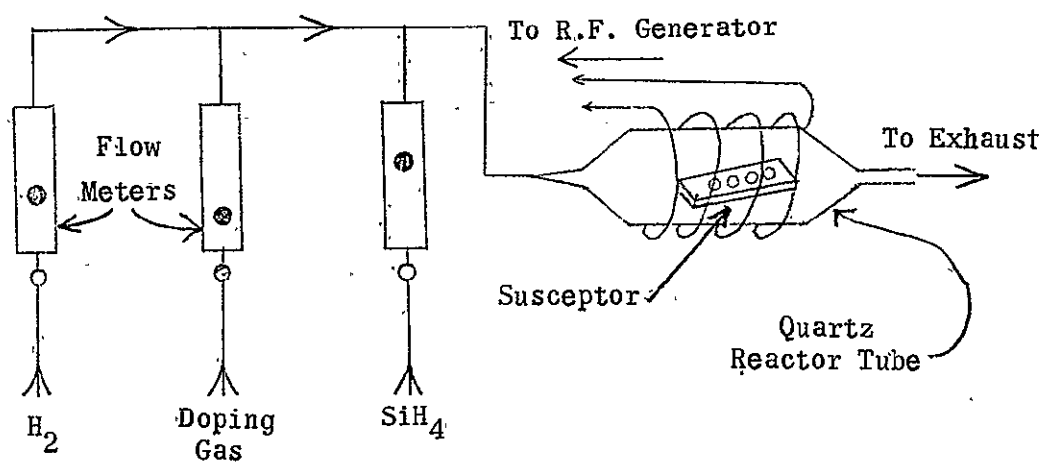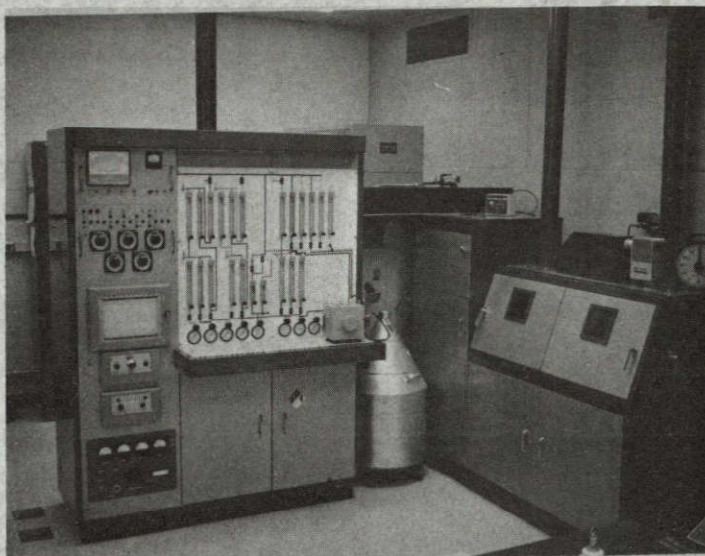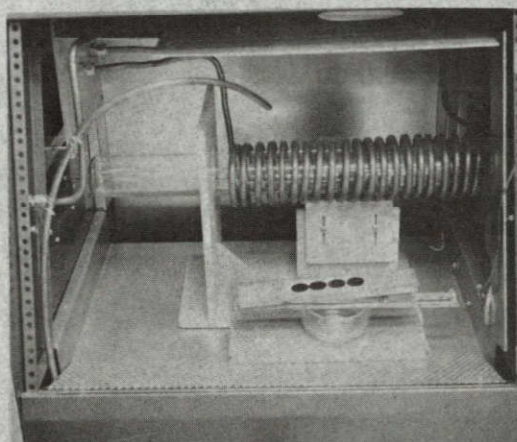cooled in hydrogen.

Figure 3.- Simplified Block Diagram of Reactor System.

(a) View of Entire System

(b) Reaction Chamber and Suscepter

Figure 4.- Reactor System.

The main hydrogen flow rate was held at a constant 13,000 cc/min for all runs. 600 cc/min of hydrogen was mixed with the SiH_4 gas immediately after the SiH_4 flowmeter on all runs. The silane gas flow rate was 50 cc/min and the deposition time was 20 minutes. This gas mixture ratio produced a very small volume percent of silane.

Volume Per Cent Silane =

$$\frac{\text{Flow rate of silane} \times 100\%}{\text{Total flow rate of all gases}} \sim \frac{\text{Flow rate of silane} \times 100\%}{\text{Flow rate of hydrogen}} =$$

$$\frac{50 \times 100\%}{13,600} = 0.37\%$$

The PH_3 flow rate, derived by two stage dilution with hydrogen, was approximately 6.5×10^{-6} cc/min. This concentration of phosphous at the given silane flow rate would produce a resistivity of 1 ohm-cm in an epitaxial silicon layer.

The lowest deposition temperature investigated was 840° C and the highest temperature was 1265° C. No meaningful results were obtained for substrate temperature greater than 1170° C.

4. Preferred Orientation Examination

At a 2θ angle of 50°, a 10μ thick silicon film offers enough mass to reduce $CuK\alpha$ X-rays to one-half intensity. Since all films to be investigated were at least 5μ thick, it was felt that X-ray diffraction would be sufficient for this phase of the research. A standard General Electric XRD-6 Powder Diffractometer was used with 50 Kv and 15 ma on the copper target tube.

The samples were 5 to 20μ thick silicon films deposited on oxidized silicon wafers which are orientated within 2° of the (111)

plane. Since both the oxide and silicon deposit are flat and parallel to the initial silicon wafer, the sample can be placed directly in the powder sample holder and the crystal planes in the deposit which are parallel to the oxide surface will be in the proper position for Bragg reflection. Generally the misorientation of the (111) plane of the silicon wafer was great enough so as not to be recorded by the diffractometer and the short range order of the SiO_2 producer to readily measurable diffraction peaks.

The preferred orientation is measured by comparing the relative intensity of the primary peaks of the sample with the relative intensities listed on the ASTM card.[25] In a sample with preferred orientation, not only does one specific X-ray diffraction peak intensity become relatively larger than that recorded on the ASTM file, but also the integrated intensity of the preferred plane may become much larger than the integrated intensity of all of the peaks combined of the randomly oriented sample. The increase in total intensity is due to the ordering of the crystals, whereas in the randomly orientated sample many crystal grains were not recorded at all since no low index face may have been normal to the axis of the X-ray goniometer.

To give accurate comparison of preferred orientations all X-ray scans were run at identical settings except for the counts-per-second (CPS) scale which, of course, is readily convertible from scale to scale. The high voltage power supply settings, beam widths, and scan speeds are listed in table II.

TABLE 2

XRD-6 X-RAY SPECTROGONIOMETER SETTINGS	
High voltage	50 KV
Current	15 ma
Beam width	1.0° medium resolution
Sollor slits	Medium resolution
Detector beam widths	0.2°
Scan speed	2° (2θ) per minute
Recorder speed	1/2 in. per minute or 4° (2θ) per inch
Counter time constant	1.0 second

5. Surface Topology Examination

X-ray diffraction measurements gave only the preferred orientation of the silicon deposits but many other important parameters were yet to be determined. In order to be useful in the dielectric isolation technique of manufacturing integrated circuits the silicon deposit had to be flat, uniform and void of pores or cracks. The deposit must also fill any and all moats or channels which were previously etched in the substrate. From a scientific viewpoint, the habit of the surface crystallites should be examined and from both a scientific and technological viewpoint, any extraneous growth, needles or spikes, should be examined.

To accomplish this surface examination both optical and scanning electron microscopy were employed. The optical microscope used was a

Bausch and Lomb Dyna Zoom Metallograph with magnification continuously variable from 80X to 800X. A Polaroid camera attachment was used to record surface features.

The scanning electron microscope (S.E.M.) is extremely useful in examining submicron surface features and its large depth of field makes it superior to the optical microscope even at ordinary magnifications. The S.E.M. (K-Square Ultrascan Model SM1) works on the principle of using magnetic lenses to produce and scan a fine beam of electrons on the specimen surface. This primary electron beam (1-20 KV) hits the specimen surface producing secondary electrons which are collected and detected by a positively biased scintillator. The output of the scintillator is displayed on a cathode-ray tube, and the primary electron beam is scanned in synchronism with the C.R.T. trace. Surface topology is revealed since the number of secondary electrons emitted is a function of the angle between the primary beam and the specimen surface.[26]

Useful magnification of the S.E.M. is from approximately 20X to 30,000X. The final magnification is a function of objective lens current and primary beam voltage and is given in the equation below:

$$X = 1.27 \times 10^4 \, KI^2 \, E^{-1/2} \tag{3.1}$$

where: X = magnification

I = Objective lens current in amperes

E = Primary beam accelerating voltage in volts

K = Magnification factor

CHAPTER IV

EXPERIMENTAL RESULTS

Introduction:

Macroscopically flat layers of polycrystalline silicon were deposited on the oxidized silicon substrates for all test temperatures except 1265° C. At a substrate temperature of 1265° C the reduction and erosion of the silicon dioxide was too rapid to hold the deposited silicon. Examination of the wafer after the run showed that all the oxide had been removed and random crystallites had nucleated and grown on the single crystal surface (Fig. 5). The remainder of this chapter will be a discussion of test results for substrate temperatures of 840 to 1170° C only.

In no tests did the etched moats (or channels) produce any irregular results but in all cases the sides and bottoms of the moats were covered with polycrystalline silicon in the same manner as the remainder of the wafer surface. The outline of the moats was still apparent after deposition but this would have been eliminated by thicker silicon deposits. Figure 6 is a photomicrograph of a cross sectioned wafer showing the filling of the moats.

All deposits were polycrystalline (test temperatures of 840 to 1170° C) with a preferred (110) orientation. The preferred orientation was strongest for substrate temperatures of approximately 1000° C.
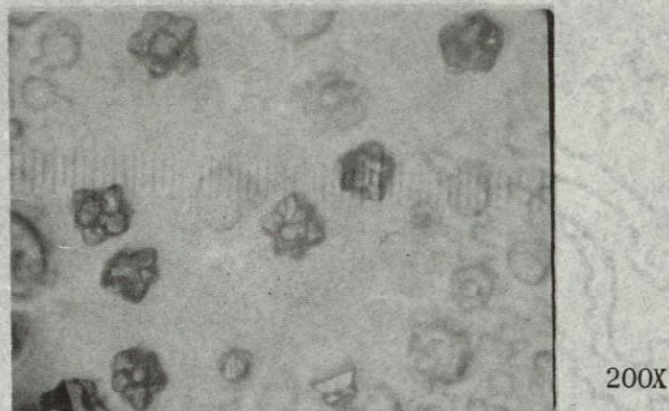
200X

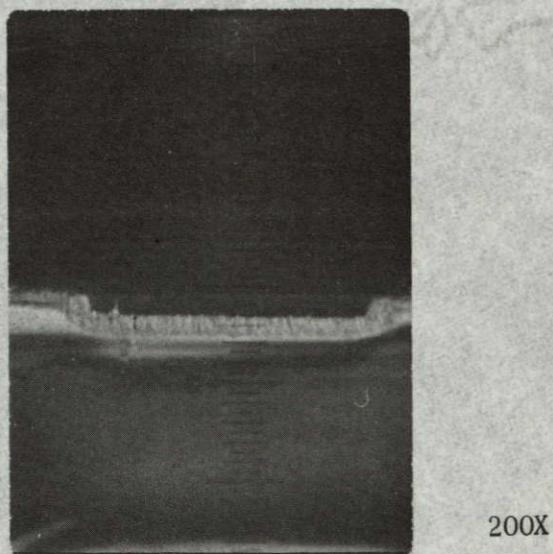Figure 5.- Crystallites on Eroded Surface.

200X

Figure 6.- Cross Section of Silicon Deposited in Etched Moat.

Preferred Orientation; General

The relative intensities of 5 low index planes of randomly orientated polycrystalline silicon are listed in the table below.

TABLE 3 (Ref. 25)

RELATIVE INTENSITIES OF LOW INDEX SILICON PLANES

Plane Index	Relative Intensity
(111)	100%
(220)*	60%
(311)	35%
(400)*	8%
(331)	17%

*Silicon, with its diamond structure, has only second order reflections for the (110) planes and fourth order reflections for the (100) planes.

The data in table 3 is from the A.S.T.M. data card which was made by X-ray diffraction of a finely divided silicon crystal. It is assumed that all crystallographic faces had an equal probability of satisfying the Bragg angle. If, in a silicon film, one or more sets of planes show a relative intensity greater than that listed on the A.S.T.M. card then the sample is said to have a preferred orientation in the direction of that set or sets of planes.

If in two sets of powdered crystals one set had a preferred orientation and one did not, then it is likely that the integrated intensity of the preferred peak would be greater than the total integrated intensity of all peaks in the randomly orientated sample. That is, preferred orientation is an ordering effect. In a preferrentially orientated sample, many crystallites which would not ordinarily contribute to any intensity peak are brought into Bragg reflection conditions.

The extent of preferred orientation, that is, the per cent of substrate surface covered by a particular orientation, can be estimated by the following model. The integrated intensity of the suspected X-ray peak of the sample is recorded and then it is compared with the integrated X-ray intensity of a single crystal, of the same material as the test sample, which is alined in the X-ray sample holder along a low index crystallographic orientation. If the deposit has a strong preferred orientation then the X-ray intensity of the sample, at the Bragg angle, should approach the intensity of the properly orientated single crystal if the same sets crystallographic planes are compared. Different sets of planes can be compared by observing the intensity ratios given on the silicon A.S.T.M. card. Only comparative measurements were used in this paper. The deposit which had the strongest X-ray intensity peak was used as a reference, but it was believed that this deposit had a very strong preferred orientation since photographs taken on the scanning electron microscope showed the surface had a very uniform texture (Fig. 13).

The per cent of preferred orientation of other planes can also be calculated from the reference sample by comparing relative intensities of the various planes listed in table 6. The equation used to calculate the percentages of preferred orientation is

$$\overline{O}_{hkl} = \frac{I_{hkl}\ (Sample)}{I\ (Reference)}\ R.I.\ (A.S.T.M.) \times 100\%$$

where:

$\overline{O}$hkl = percentage of crystallites of which the (hkl) plane that lies parallel to substrate surface (as compared to the reference sample)

I_{hkl}
(Sample) = X-ray intensity of the (hkl) plane of the sample being
　　　　　investigated.

I (Reference) = X-ray intensity of reference sample = 2600 cps

R.I.(A.S.T.M.) = Relative intensity, as obtained from the standard
　　　　　　　A.S.T.M. file card, of the (hkl) plane and the plane
　　　　　　　of orientation of the reference sample.

Results:

The crystallography of the deposits was strongly temperature dependent. The absolute intensity of the (220) crystal peak shows an increase with increasing temperature until 1000° C and then the (220) intensity decreased with further increases in temperature (Fig. 7). As may be expected, the relative (to the (220) peak) intensities of the other low index crystallographic planes increased as the absolute (220) intensity decreased (Figs. 8-11), indicating that the orientation of the
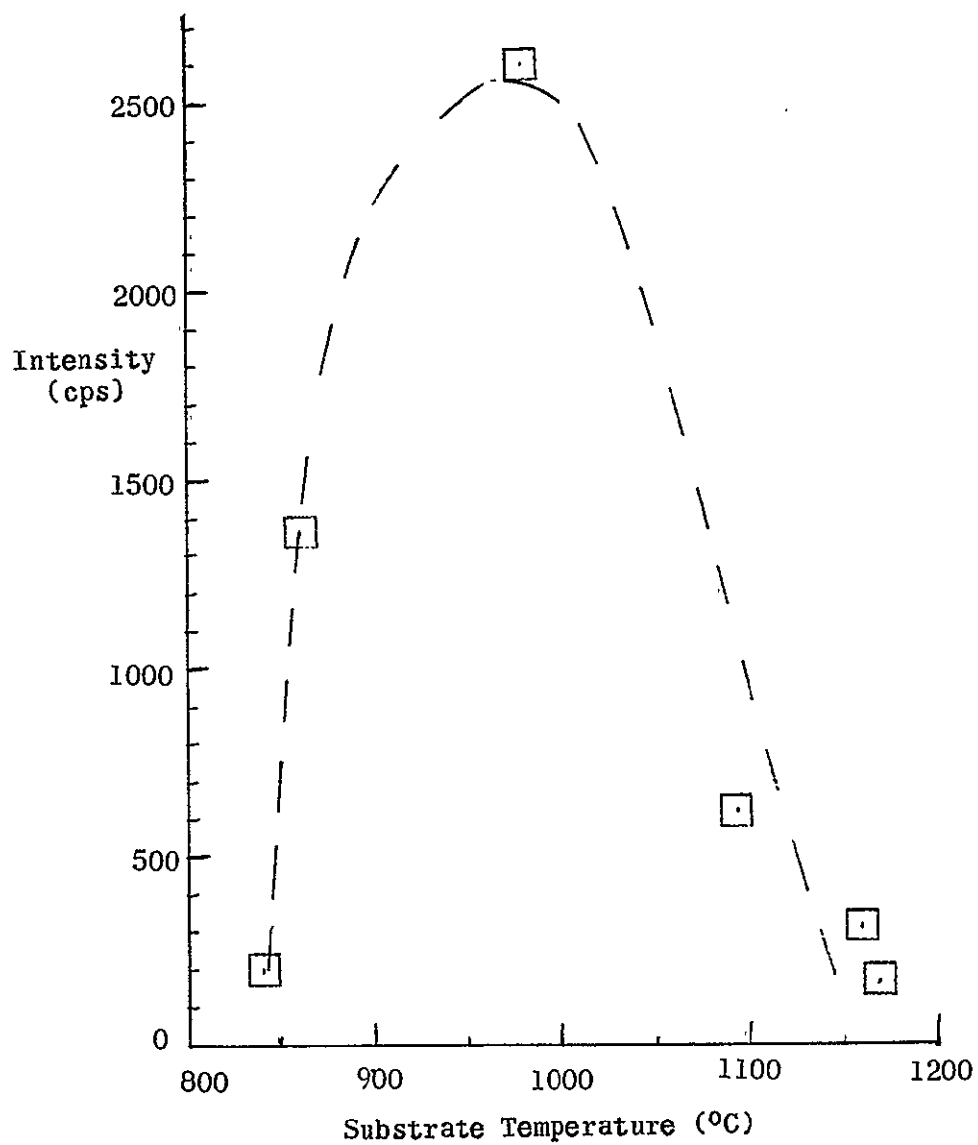
Figure 7.-

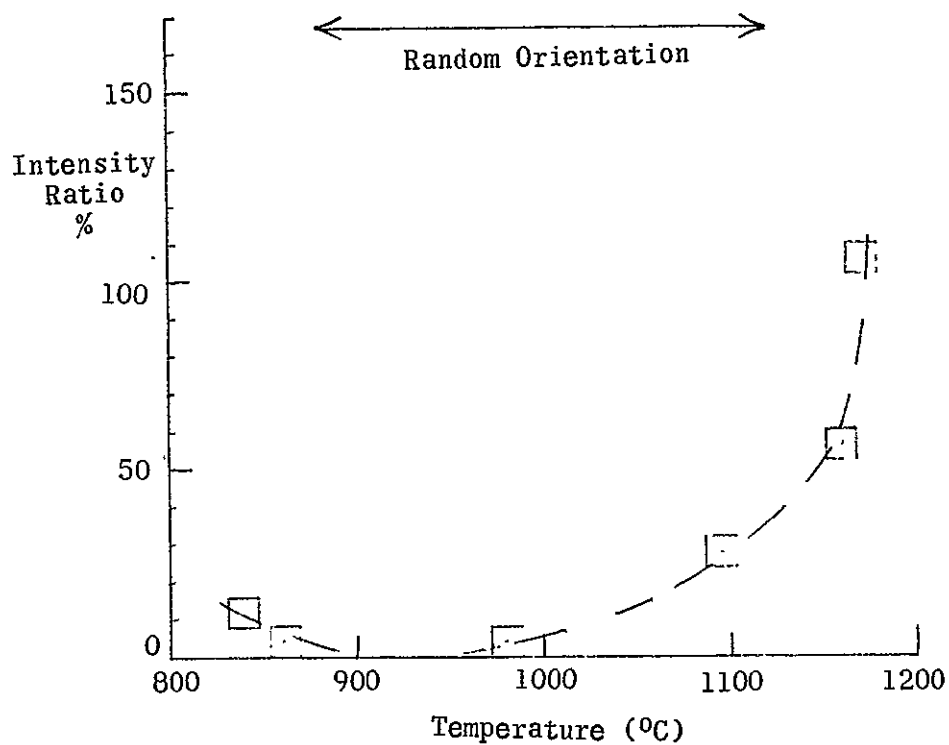Intensity of (220) Diffraction Peak vs. Substrate Temperature.

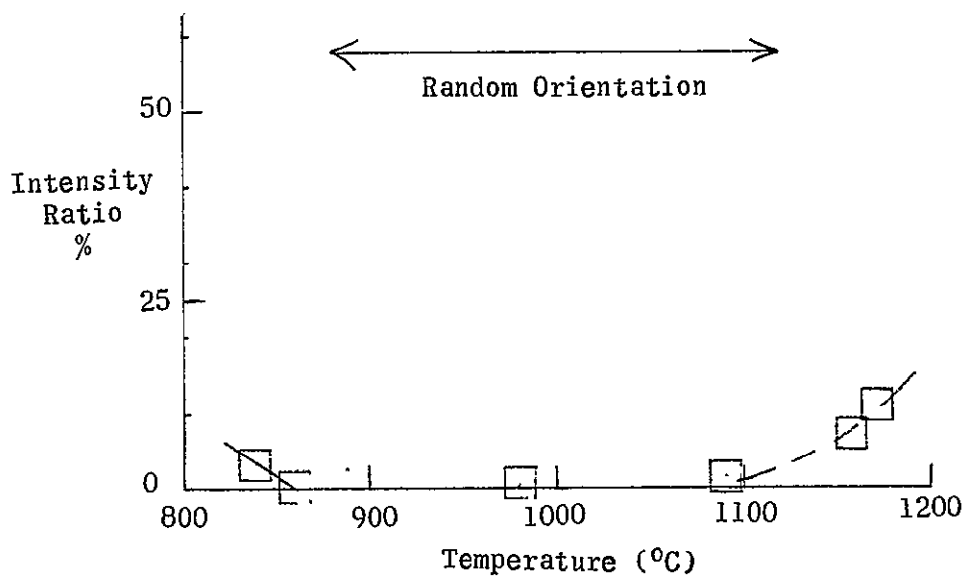Figure 8.- (111)/(220) Intensity Ratio vs. Substrate Temperature.

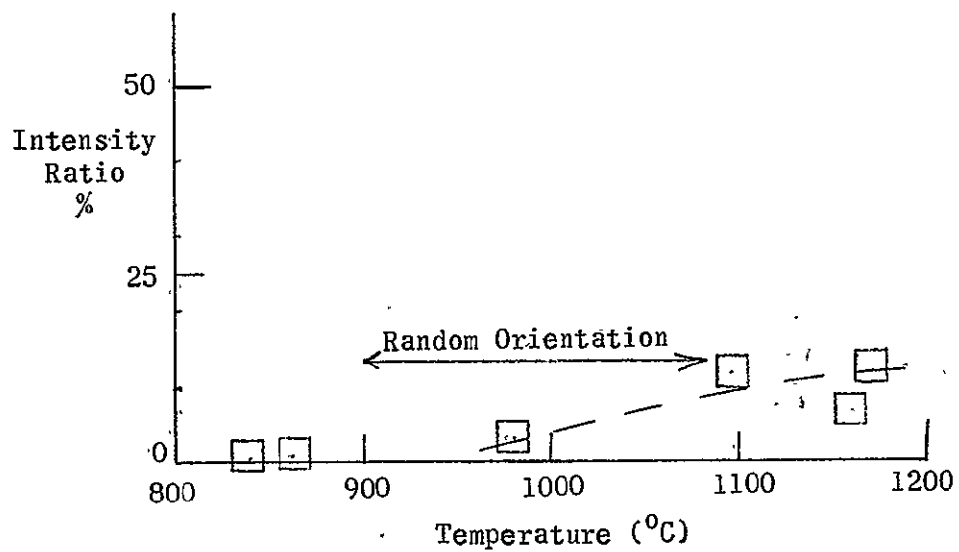Figure 9.- (311)/(220) Intensity Ratio vs. Substrate Temperature.

Figure 10.- (400)/(220) Intensity Ratio vs. Substrate Temperature.
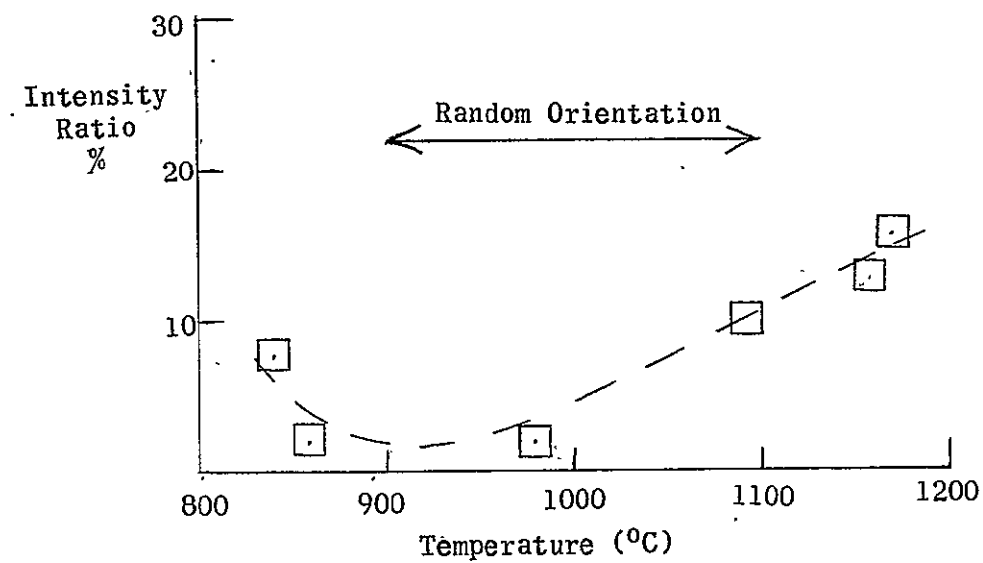

Figure 11.- (331)/(220) Intensity Ratio vs. Substrate Temperature.

deposit was going from a strong preferred orientation to a more random orientation. Table 4 tabulates the X-ray data in terms of the absolute (220) intensity and relative intensities of the other planes. The per cent of deposited crystallites which have either their (111), (110), (100), or (331) faces alined parallel to the substrate surface is calculated by using equation 4.1 and the results are listed in table 5. (The data tabulated in table 5 is not exact, since no standard was used as reference, but it is only comparative data, since sample 2-3 which had a very strong (220) line and very low relative intensities of other planes were used as the reference.)

The X-ray data indicates that the deposits go from a very strong preferred (110) orientation at approximately 1000° C to an almost equally mixed, but moderately strong, preferred orientations of (110) and (100) crystallites at approximately 1100° C and then to an almost random or mixed orientation at deposition temperatures near 1200° C. Even in the high temperature deposits the (111), (311), and (331) orientations are depressed from the standard A.S.T.M. (relative to the (220) peak) intensities; hence, the deposits are not completely random but still have a slight (110) and (100) preferred orientation with the (110) orientation dominating in all runs.

The lowest temperature deposit made was at 840° C. The absolute (220) amplitude was no lower than some high temperature depositions (see table 4) but the relative amplitudes of the other planes were lower for this sample than for the high temperature depositions (see Figs. 9-12). The low absolute amplitude of the (220) peak is not
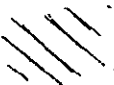
TABLE 4

X-RAY DIFFRACTION RESULTS
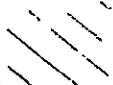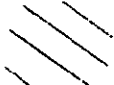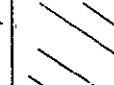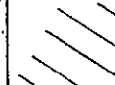
Sample	2-1	2-2	2-3	2-4	2-5	2-6	ASTM
Temperature (°C)	840	860	980	1095	1160	1170	---
Intensity of (220) (cps)	195	1360	2600	620	300	160	---
Intensity of (111) (% of (220))	11	b	b	26	55	105	167
Intensity of (311) (% of (220))	3	n	n	b	7	10	58
Intensity of (400) (% of (220))	n	n	3	12	7	12	13.5
Intensity of (331) (% of (220))	7.5	2	2	10	13	16	22

b = detectable, but not measurable, on range of which data was obtained.

n = not detectable on range of which data was obtained.

TABLE 5

COMPARISON OF PER CENT PREFERRED ORIENTATION OF LOW INDEX PLANES IN
SILICON DEPOSITS USING THE (220) INTENSITY OF
SAMPLE 2-3 AS A STANDARD

Sample	2-1	2-2	2-3	2-4	2-5	2-6
Temperature $^\circ$ C	840	860	980	1095	1160	1170
Plane index						
(111) (%)	1	b	b	3.7	3.8	3.9
(110) (%)	7.3	52	100	24	11	6.2
(100) (%)	n	n		21	6	5.5
(331) (%)	2.5	5		11	7	4.5
Surface covered by preferred growth (%)	10	57		56	28	20
(220) intensity (cps)	195	1,360	2,600	620	300	160

b = detectable, but not measurable, on range of which data was obtained

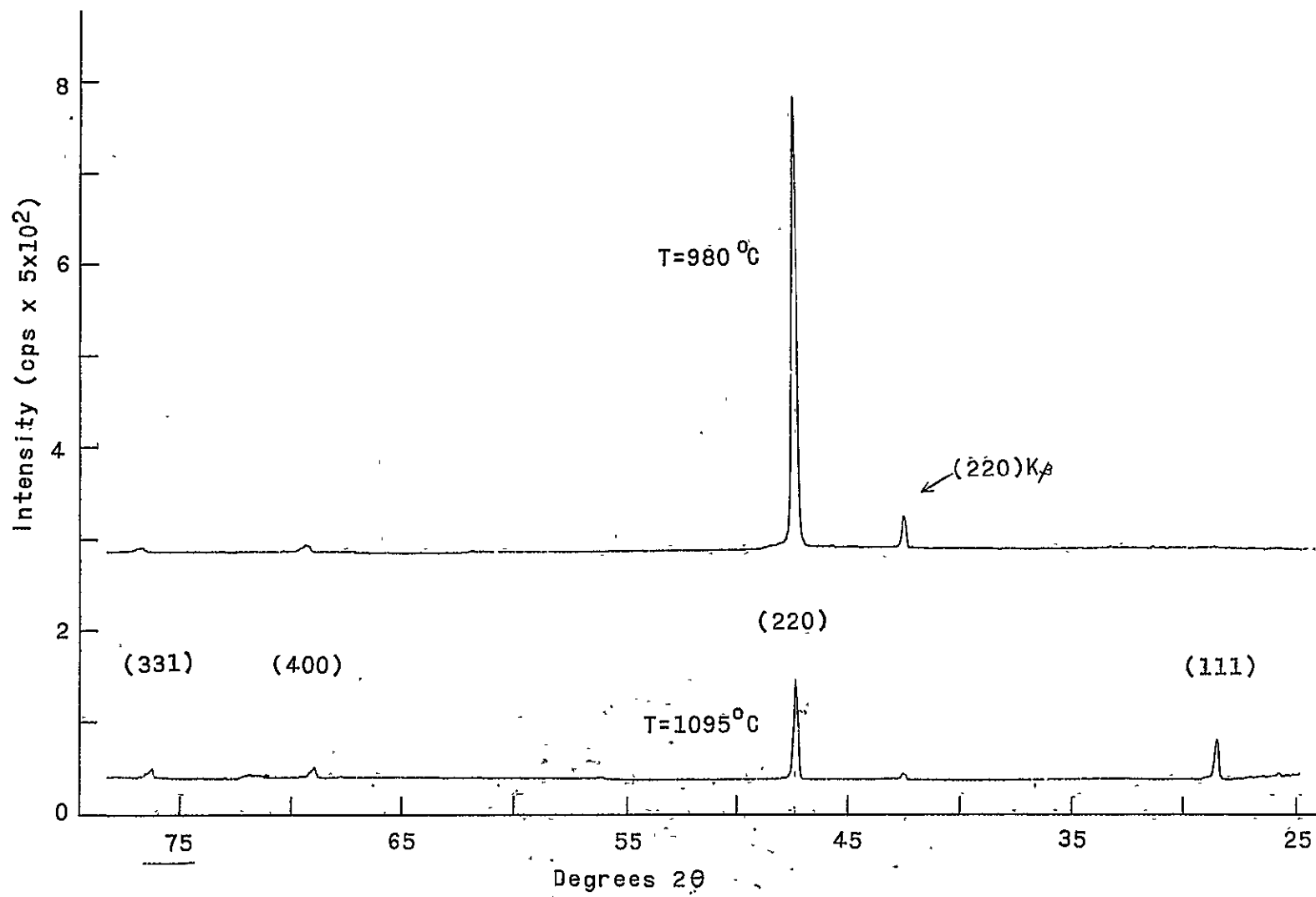n = not detectable on range of which data was obtained.

Figure 12.- Diffraction Intensity vs. Bragg Angle.

explained in terms of the deposit going to a random orientation. Using silane, amorphous silicon has been deposited on glass substrates at temperatures as high as 650° C, and the macroscopic appearance resembled the crystalline form.[27] Hence, this deposit is probably mostly amorphous and the crystallites that do exist have a preferred (110) orientation.

An example of the X-ray diffractometer data is shown in Figure 12 where the diffraction peaks from sample 2-3 are compared to the peaks in sample 2-4. Both diffraction patterns were taken with identical machine settings. The upper curve shows a very strong (220) peak and the lower curve shows a weaker (220) peak, but the relative (and in this case, the absolute) intensities of the (111), (400) and (331) peaks have increased.

The surface topology of the samples was examined by using both an optical microscope and a scanning electron microscope. The majority of the surface of all samples was covered with small (≈ 1μ), slightly rounded crystallites (see Figs. 13 and 14). Scattered about on some samples were random growths of spikes or needles. The extraneous growths were most common on the lower temperature deposits, but no general pattern or condition for growth was observed.

The appearance of the small crystallites which covered most of the surface varied slightly with temperature. Sample 2-3 has been determined, by X-ray diffraction, to be almost completely covered with crystallites orientated with the (110) face parallel to the surface, and the photomicrograph taken with the scanning electron microscope (Fig. 13) shows that nearly all crystallites are similar in appearance as though

there is a common morphology for the (110) orientation. Sample 2-4
has been determined to have a mixed orientation of (110) and (100)
planes (the (110) dominates) with a representation of other orientations
as well (table 5.). Examination of the magnified surface shows a large
number of crystallites which were common to the (110) orientation and
also a number of other shapes, one of which is characteristic of a (100)
orientated octahedron (Fig. 14).

Summary of the Experimental Results:

The microstructure of the deposited silicon films was strongly
dependent on substrate temperature. At the lowest substrate temperature
the deposit was nearly amorphous with the existing crystallites alined
in the (110) direction. As the deposition temperature increased toward
1000° C, the deposit became more crystalline with the majority of
crystallites alined with their (110) face parallel to the substrate.
Above 1000° C the extent of preferred (110) orientation decreased and
there was a significant contribution from (100) orientated crystallites.
At temperatures near 1200° C the deposits are nearly random with a weak
(110) and (100) preferred orientation with the (110) orientation
dominating.

The diameter of the deposited crystallites was approximately 1μ
on all samples. The morphology of these crystallites could be correlated
with the extent of preferred orientation of the deposited films.

(a) 960X
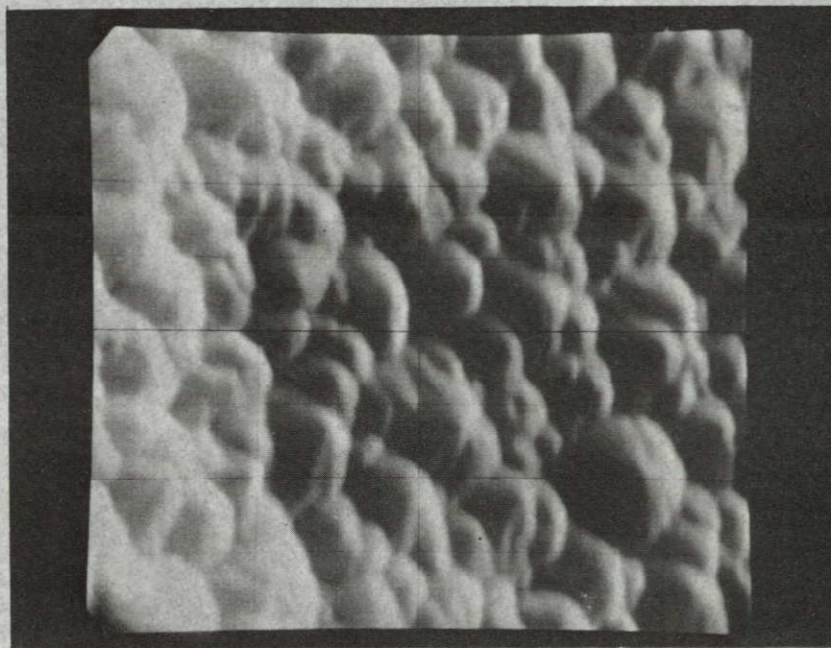
(b) 4800X

Figure 13.- S.E.M. Photomicrographs of Sample 2-3, T = 980° C.
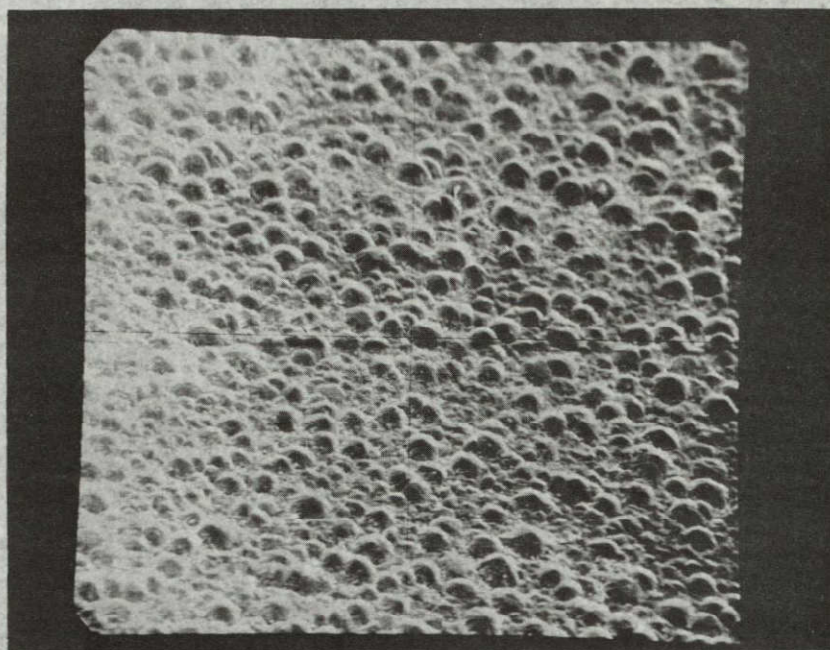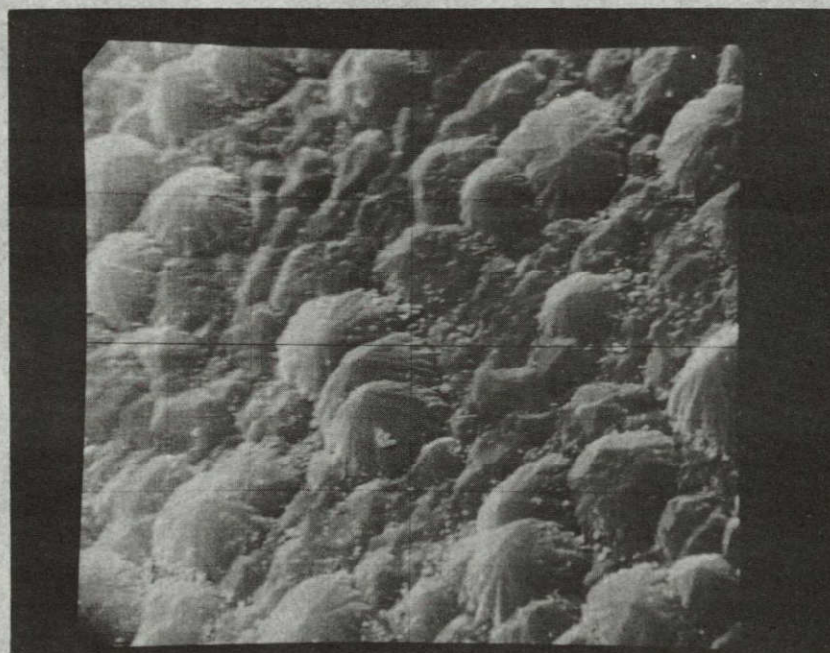
(a) 700X

(b) 3500X

Figure 14.- S.E.M. Photomicrographs of Sample 2-4, T = 1095° C.

CHAPTER V

EXPLANATION OF RESULTS

It has been demonstrated that in silicon on silicon epitaxial
growth an orientated nucleus on the (111) surface is stable with three
atoms[15] and nucleation on a (100) surface is stable with four atoms.[17]
The results were obtained by fitting data to extrapolated theory
originally developed by Lewis and Campbell.[7] However, this data was
obtained on substrates where initial nucleation started at what was
postulated as being points of carbon contamination,[17] hence, these
minimum nuclei models would not necessarily carry over to other
substrates. That is, the minimum stable (111) nucleus is three atoms
when nucleation begins at a point of carbon contamination. The minimum
nucleus for a perfect (111) surface is not known. Hence, it is not
conclusive that all (111) orientated silicon growths begin as three
atom nuclei.

Bicknell[5] has proposed a model for silicon epitaxy on crystalline
quartz. In this model the SiO_2 substrate surface becomes oxygen deficient
during high temperature treatment in a hydrogen atmosphere and the
surface silicon atoms (in the quartz) have free bonds to attach to the
depositing silicon atoms. The silicon atoms in the (10$\bar{1}$0) surface of
quartz are alined such that there is only a small misfit from the (100)
silicon crystal planes and bonding in the quartz is such that in an
oxygen reduced (10$\bar{1}$0) surface there would be two bonds exposed per
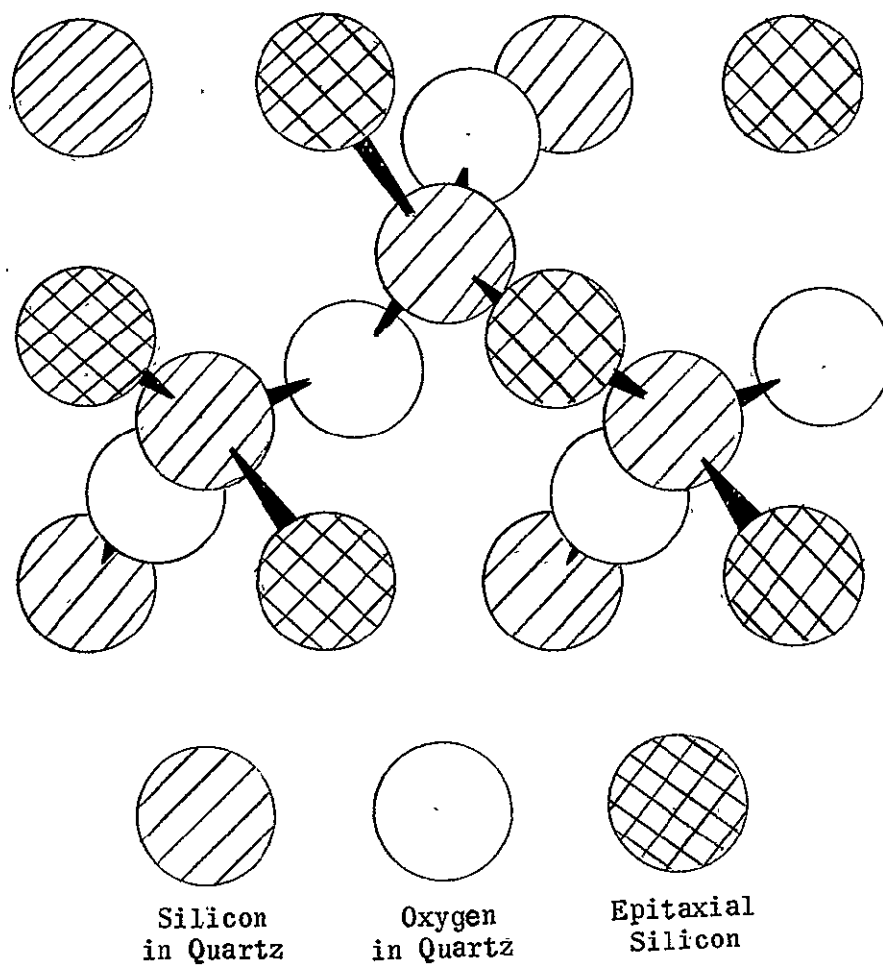silicon atom (Fig. 15). In (100) orientated silicon there are two

Figure 15.- Silicon on Quartz Epitaxy (Reference 5).

silicon bonds from each atom going to atoms in the plane above the
plane of reference.

By extrapolating Bicknell's model to amorphous SiO_2 with short
range cristobalite structure in which the silicon atoms have an average
interatomic spacing of 3.1 Å,[22] the following model is proposed. The
surface is again made oxygen deficient due to high temperature treatment
in a hydrogen atmosphere and silicon bonds are exposed on the surface.
If short range order exists in the silicon dioxide and the average
silicon-silicon interatomic spacing is 3.1 Å as measured by Pavlov and
Shitova,[22] then it is reasonable to expect the surface to have a typical
configuration of two exposed silicon atoms 3.1 Å apart with a third
exposed silicon atom 3.1 Å from the second atom, at an arbitrary angle
from the line between the first two atoms but spaced not less than
3.1 Å from the first atom (see Fig. 16). This, of course, is the
configuration for any three adjacent silicon atoms and the configuration
is repeated again and again across the silicon dioxide surface. The
angle of the third atom changes from group to group. The density of
exposed silicon atoms, and hence, the density of the triads, will
increase as temperature increases. Therefore, random distribution of
second neighbor silicon atoms as constrained above will produce possible
bonding sites at all spacings between 3.1 Å and 6.2 Å.

Figure 17 identifies the planar interatomic spacings of the (111),
(110), and (100) planes of silicon and table 6 lists the spacings with a
±15 per cent tolerance which is often considered maximum for orientated
overgrowth. This information suggests that there are six different ways
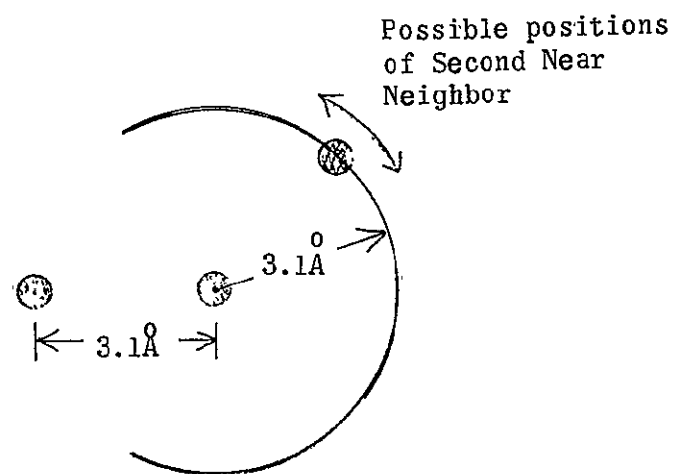
Figure 16.- Locus of Possible Second Near Neighbor Positions
in Amorphous Cristobalite.
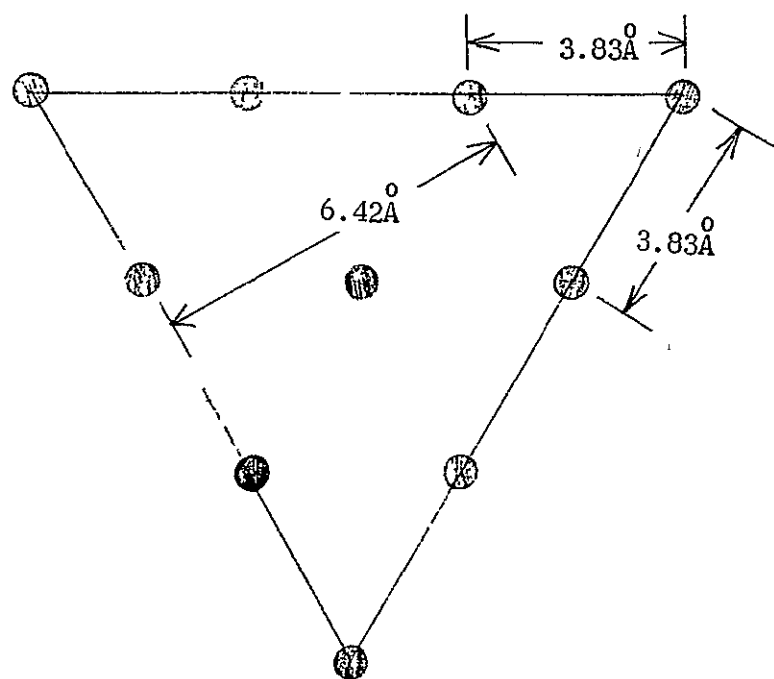
Figure 17a.- Planar Interatomic Spacing of (111) Silicon.
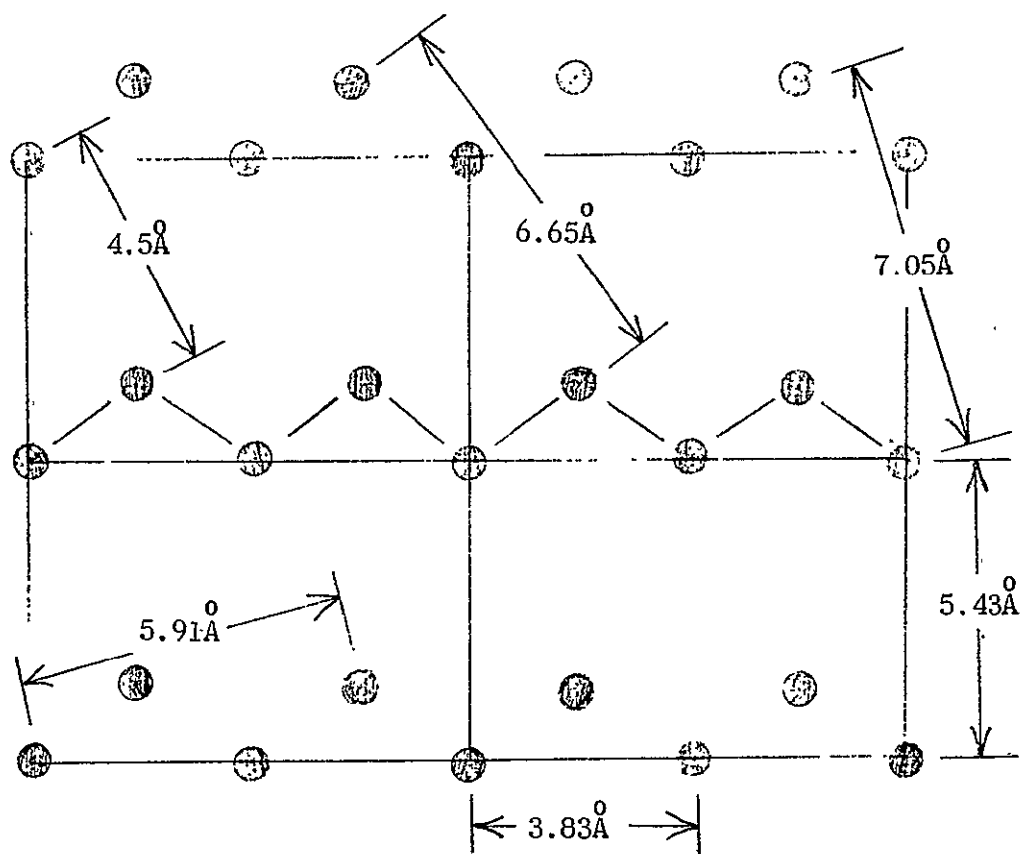
Figure 17b.- Planar Interatomic Spacing of (110) Silicon.
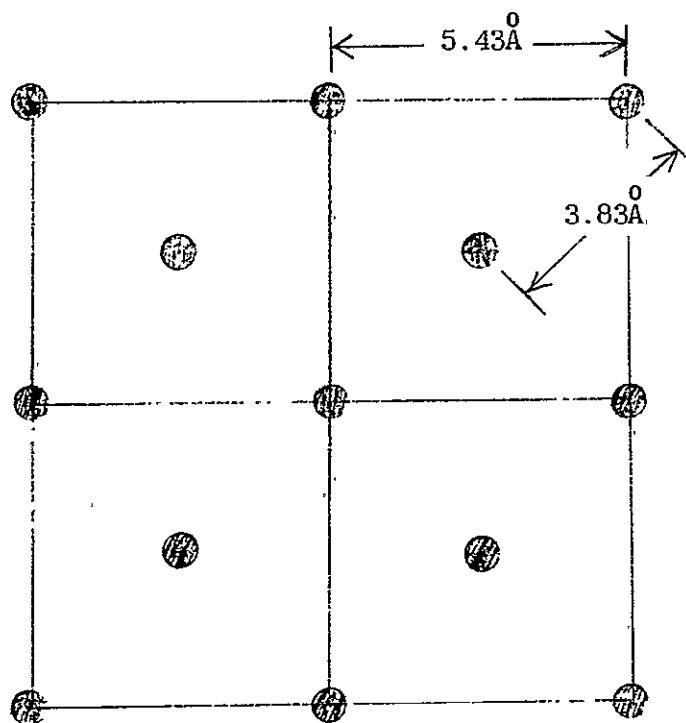
Figure 17c.- Planar Interatomic Spacing of (100) Silicon.

TABLE 6

INTERATOMIC DISTANCES (WITHIN THE PLANE) FOR LOW INDEX
ORIENTATIONS OF SILICON

(111)		(110)		(100)	
d (Å)	d + 15% (Å)	d (Å)	d + 15% (Å)	d (Å)	d + 15% (Å)
3.83	3.25 - 4.4	3.83	3.25 - 4.4	3.83	3.25 - 4.4
6.42	5.46 - 7.38	4.5	3.8 - 5.3	5.43	4.6 - 6.2
		5.43	4.6 - 6.2		
		5.91	5.0 - 6.8		
		6.65	5.65 - 7.65		
		7.05	6.0 - 8.1		

of fitting a (110) orientation on the short range order SiO_2 compared to two each for the (111) and (100) orientations.

It seems reasonable to expect that not only the number of ways to make an orientated fit will contribute to the probability of a given orientation but that the length along the third atom locus which falls within ±15% of the interatomic spacing will also contribute to the orientation probability. That is, if the third silicon atom in the triad is considered to lie at a random position on the curve in Figure 16, then the length along the curve which would accommodate a certain orientation should be a relative probability of obtaining that orientation.

The equation for the length along the third atom locus is:

$$ S = 2A \left\{ \cos^{-1}\left(\frac{d^2_{min}}{2A^2} - 1\right) - \cos^{-1}\left(\frac{d^2_{max}}{2A^2} - 1\right) \right\} . $$

where:

S = distance along third atom locus which is within ±15 per cent of the interatomic distance of a particular set of silicon atoms in a particular orientation

A = average silicon-silicon interatomic spacing in thermal silicon dioxide = 3.1 $\overset{o}{A}$.

d min = Interatomic spacing (-15%) of the particular set of silicon atoms referred to in the definition of S.

d min $\geq$ 3.1 $\overset{o}{A}$.

d max = Interatomic spacing (+15%) of the particular set of

silicon atoms referred to in the definition of S.

d max ≤ 6.2 $\overset{o}{A}$.

The lengths along the third atom locus for each possible
interatomic spacing is listed in table 7.

TABLE 7

LENGTH ALONG THE THIRD ATOM LOCUS FOR LOW INDEX ORIENTATIONS
OF SILICON

(111)		(110)		(100)	
d $(\overset{o}{A})$	S $(\overset{o}{A})$	d $(\overset{o}{A})$	S $(\overset{o}{A})$	d $(\overset{o}{A})$	S $(\overset{o}{A})$
3.83	2.86	3.83	2.86	3.83	2.86
6.42	6.14	4.5	4.50	5.43	9.16
		5.43	9.16		
		5.91	7.84		
		6.65	5.28		
		7.05	3.10		

The number of bonds needed from the surface silicon atoms to

induce a given orientation also needs to be considered. Silicon planes

alined in a (110) orientation have one bond per atom going from one

plane to the next; where as planes alined in either the (111) or (100)

orientations have two bonds per atom going from one plane to the next

plane. That is, only the (110) orientation has adjacent atoms in the

plane. Since the model is based on a surface which is made oxygen
deficient due to hydrogen reduction at high temperatures, it is likely
that at the lower deposition temperatures there will be a higher density
of single exposed bonds than would exist at the higher test temperatures.
Hence, in just considering the number of bonds needed for nucleation
orientation the higher temperatures would be more conducive to (111)
and (100) orientations than to (110) orientations.

Hence, considering the lengths along the third atom position
curve and the number of ways of alining the various orientations, and
the temperature effects of freeing surface silicon bonds the following
should be expected:

1. (110) orientation at lower temperatures

2. (110) and (100) orientations as temperature rises

3. Random orientation at very high temperatures

In crystalline, cristobalite the second silicon-silicon inter-
atomic distance is 5.03 $\overset{o}{A}$. Pavlov and Shitova[22] did not publish data
showing the cristobalite structure in thermal SiO_2 extending to three
silicon atoms, but if the "amorphous" SiO_2 structure did extend past
near neighbors only, there would still be conditions for nucleation
orientation. The same argument as before is used for the production
of free silicon bonds but now the interatomic distances for the various
orientations are compared to a fixed 5.03 $\overset{o}{A}$ instead of to all points
along the curve in Figure 16. Looking back at table 6, it is seen that
there are now three ways to fit a (110) orientated nucleus on the

surface, one way to fit a (100) orientated nucleus on the surface and no way to fit a (111) orientated nucleus.

This model still predicts a (110) orientated deposit at lower temperatures and (110) and (100) orientations as the temperature rises, but it does not predict the emergence of (111) orientated growth. If this model is correct, then the nucleation of (111) and other orientations could start in disordered regions of the reduced silicon dioxide. Hence, either model of the silicon dioxide surface produces the same qualitative results.

REFERENCES

1. Thompson Rano Wooldridge, Inc., Redondo Beach, California: United States Air Force Contract Report; AF 33(615) - 1949 (Nov. 1964), "High Impedance Isolation Techniques for Monolithic Circuit Structures."

2. Maxwell, D. A.; Beeson, R. H.; and Allison, D. F.: "The Minimization of Parasitics in Integrated Circuits by Dielectric Isolation." IEEE Transactions on Electron Devices, vol. ED-12, p. 20 (1965).

3. Jackson, D. M.: "Advanced Epitaxial Processes for Monolithic Integrated-Circuit Applications." Transaction of the Metallurgical Society of AIME, vol. 233, p. 596 (1965).

4. Breckenridge, R. G.: Union Carbide Corp., Parma, Ohio; United States Army Contract No. DA 36-039 SC-90734, Project No. 3A99-21-001; AD 418340 (May 1963), "Active Thin-Film Circuit Functions."

5. Bicknell, R. W.; Charig, J. M.; Joyce, B. A.; and Stirland, D. J.: "The Epitaxial Deposition of Silicon on Quartz." Philosophical Magazine, vol. 9, p. 965 (1964).

6. Runyan, W. R.: "Electronic Materials." Vapor Deposition, p. 593; edited by C. F. Powell, J. H. Oxley, and J. M. Blocher, Jr.; John Wiley and Sons, Inc., New York, 1966.

7. Lewis, B.; and Campbell, D. S.: "Nucleation and Initial-Growth Behavior of Thin-Film Deposits." The Journal of Vacuum Science and Technology, vol. 4, p. 209 (1967).

8. Rhodin, T. N.; and Walton, D.: "Nucleation of Oriented Films." Single Crystal Films, p. 31; edited by M. H. Francombe and H. Sato; The Macmillan Company, New York, 1964.

9. Collins, F. M.: "Vacuum Evaporated Silicon Films." Transactions of the Eighth National Vacuum Symposium, vol. 2, p. 899; edited by L. E. Preuss; The Macmillan Company, New York, 1961.

10. Katooka, Y.: "Some Properties of Evaporated Silicon Films." Journal of the Physical Society of Japan, vol. 17, p. 967 (1962).

11. Morentvala, A. J.; and Abowitz, G.: "Textural Characteristics and Electrical Properties of Vacuum Evaporated Silicon Films." Vacuum, vol. 15, p. 359 (1965).
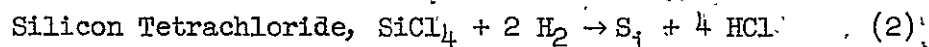
12. Kumagoi, H. Y.; Thompson, J. M.; and Krauss, G.: "Properties and Structure of Thin Silicon Films Sputtered on Fused Quartz Substrates," Transactions of the Metallurgical Society of AIME, vol. 236, p. 295 (1966).

13. Alexander, E. G.; and Runyan, W. R.: "A Study of Factors Affecting Silicon Growth on Amorphous SiO_2 Surfaces," Transactions of the Metallurgical Society of AIME, vol. 236, p. 284 (1966).

14. Bylander, E. G.; and Mitchell, M. M.: "Progress on Device Formation in Silicon Pyrocrystallites on Insulating Substrates." Metallurgy of Advanced Electronic Devices, vol. 19, p. 293; edited by G. E. Brock; Interscience Pub., New York, 1962.

15. Joyce, B. A.; and Bradley, R. R.: "A Study of Nucleation in Chemically Grown Epitaxial Films Using Molecular Beam Techniques; III. Nucleation Rate Measurements and the Effect of Oxygen on Initial Growth Behavior." Philosophical Magazine, vol. 15, p. 1167 (1967).

16. Booker, G. R.; and Joyce, B. A.: "A Study of Nucleation in Chemically Grown Epitaxial Silicon Films Using Molecular Beam Techniques; II. Initial Growth Behavior on Clean and Carbon-Contaminated Silicon Substrates." Philosophical Magazine, vol. 14, p. 301 (1966).

17. Joyce, B. A.; Bradley, R. R.; and Watts, B. E.: "A Study of Nucleation in Chemically Grown Epitaxial Silicon Films Using Molecular Beam Techniques; V. Nucleation Kinetic Measurements on (100) Surface." Philosophical Magazine, vol. 19, p. 403 (1969).

18. Joyce, B. A.; and Bradley, R. R.: "Epitaxial Growth of Silicon From the Pyrolysis of Monosilane on Silicon Substrates." Journal of the Electrochemical Society, vol. 110, p. 1235 (1963).

19. Mayer, S. E.; and Shea, D. E.: "Epitaxial Deposition of Silicon Layers by Pyrolysis of Silane." Journal of the Electrochemical Society, vol. 111, p. 550 (1964).

20. Bhola, S. R.; and Mayer, A.: "Epitaxial Deposition of Silicon by Thermal Decomposition of Silane." RCA Review, vol. 24, p. 511 (1963).

21. Joyce, B. A.; Bennett, R. J.; Bicknell, R. W.; and Etter, P. J.: "The Epitaxial Deposition of Silicon on Quartz and Alumina." Transactions of the Metallurgical Society of AIME, vol. 233, p. 556 (1965).

22. Pavlov, P. V.; and Shitova, E. V.: "Electron Diffraction Investigation of the Structure of SiO_2 Films Obtained by Different Methods." <u>Soviet Physics - Crystallography</u>, vol. 12, p. 95 (1967).

23. Knopp, A. N.; and Stickler, R.: "The Structure and Perfection of Thermally Grown Oxide Films on Silicon." <u>Electrochemical Technology</u>, vol. 5, p. 37 (1967).

24. <u>Integrated Circuits, Design Principles and Fabrication.</u> p. 371; edited by R. M. Warner, Jr.; McGraw-Hill Book Co., New York (1965).

25. ASTM Card. No. 5-0565, American Society for Testing Materials, Philadelphia, Pa.

26. R. F. W. Pease: "The Scanning Electron Microscope." <u>IEEE Spectrum</u>, vol. 4, p. 96 (1967).

27. Chittick, R. C.; Alexander; and Sterling, H. F.: "The Preparation and Properties of Amorphous Silicon." <u>Journal of the Electrochemical Society</u>, vol. 116, p. 77 (1969).

28. <u>Matheson Gas Data Book.</u> The Matheson Co., Inc. (1966).

29. Armirotto, A. L.: "Silane: Review and Applications." <u>Solid State Technology</u>, p. 43 (Oct. 1968).
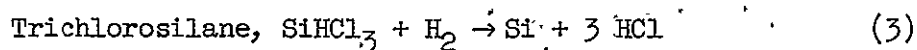
APPENDIX I

1. PROPERTIES OF SILANE (SiH_4)[19,20]

Silane is a colorless, pyrophoric gas which breaks down into its elemental components at temperatures as low as 400° C. There are no corrosive byproducts in the pyrolytic reaction as there are in the hydrogen reduction of silicon tetrachloride and trichlorosilane; that is, the basic reactions are

$$\text{Silane, } SiH_4 \rightarrow Si + 2 H_2 \tag{1}$$

$$\text{Silicon Tetrachloride, } SiCl_4 + 2 H_2 \rightarrow S_i + 4 HCl \tag{2}$$

and

$$\text{Trichlorosilane, } SiHCl_3 + H_2 \rightarrow Si + 3 HCl \tag{3}$$

The HCl byproduct of reactions (2) and (3) is highly corrosive and in silicon on silicon epitaxial deposition a net etching may result.

Under clean laboratory conditions, the standard grade of silane is capable of producing silicon on silicon epitaxial layers with a resistivity of better than 50 ohm-cm, which corresponds to a net impurity doping level of the order of one part per 10^8 silicon atoms. The physical properties of silane are listed in table 8.

TABLE 8

PHYSICAL PROPERTIES OF SILANE[20]

Molecular weight 32.12

Specific volume at 70° F, 1 atm. . . . .   12.1 cu ft/lb

Boiling point at 1 atm. . . . . -112° C

Freezing point at 1 atm. . . . . : -185° C

Density, gas at 20° C 1.44 g/1

Specific gravity, liquid at -185° C . .   0.68

Critical temperature . . . . -4° C

Critical pressure . . . .   702.7 psia (47.8 atm.)

Viscosity at 15° C . . . .   112.4 micropoise

APPENDIX II

MATERIALS USED IN EXPERIMENTS

Gases, chemicals, and crystals, were all high quality semiconductor
grade materials capable of being used in construction of semiconductor
devices. The materials used are listed below along with their primary
function, purity, and source.

TABLE 9

Item	Function	Grade or impurity	Source
Silicon wafers	Substrate for silicon outside growth	*0.005 ohm-cm boron doped	Electronic Materials, Incorporated
Silane (SiH_4)	Silicon deposition	*50 ohm-cm	Matheson Gas Products
Hydrogen (H_2)	Carrier gas for silane	Purified in liquid nitrogen cold trap	Government stock
Phosphine (PH_3)	Doping gas	Diluted in H_2 100 ppm impurities, < 10 ppm	Matheson gas products
Nitric acid (HNO_3)	(a) Cleaning wafers (b) Silicon etch	Reagent A.C.S.	Fisher Sci. Co.
Hydrofluoric acid (HF)	(a) Oxide etching (b) Silicon etching	Reagent A.C.S.	Fisher Sci. Co.

Item	Function	Grade or impurity	Source
Glacial Acetic acid (CH_3COOH)	Silicon etching	Reagent A.C.S.	Fisher Sci. Co.
Ammonium Fluoride (NH_4F)	Oxide etching	Certified	Fisher Sci. Co.
Trichloroethylene	Cleaning wafers	Electronic grade	Fisher Sci. Co.
Methanol	Cleaning wafers	Spectro-analyzed	Fisher Sci. Co.
Water	(a) Oxygen source for oxide process (b) Cleaning wafers (c) Dissolving NH_4F	Distilled & deionized	Local still

*The resistivity of a semiconductor is not a true or exact indicator of crystal purity, but it is an indicator of the net electrically active impurity atoms. The resistivity of pure, intrinsic, silicon has been calculated to be approximately 230,000 ohm-cm, at 300° K and if one could start with pure silicon and add one boron atom for every 10^8 (10^4) silicon atoms the resistivity would drop to 50 ohm-cm (0.005 ohm-cm). In practice, however, the resistivity of the silicon sample is only a measure of the difference in number of p-type and n-type impurity atoms.

DEPOSITION AND EVALUATION OF SILICON FILMS FORMED BY PYROLYTIC DECOMPOSITION OF SILANE ON OXIDIZED SILICON SINGLE CRYSTALS

Archibald Linley Fripp, Jr.

Virginia University
Charlottsville, Virginia

June 1969